Selective, Controllable, and Reversible Aggregation of Polystyrene Latex Microspheres via DNA Hybridization

Phillip H. Rogers,[†] Eric Michel,[‡] Carl A. Bauer,[†] Stephen Vanderet,[†] Daniel Hansen,[†] Bradley K. Roberts,[§,∥] Antoine Calvez,[†] Jackson B. Crews,[†] Kwok O. Lau,[§] Alistair Wood,[†] David J. Pine,[‡,£,⊥] and Peter V. Schwartz*[,†]

Physics Department, California Polytechnic State University, San Luis Obispo, California 93407, Chemical Engineering Department, University of California, Santa Barbara, California 93106-5080, Materials Engineering Department, California Polytechnic State University, San Luis Obispo, California 93407, and Materials Department, University of California, Santa Barbara, California 93106

Received December 25, 2004. In Final Form: April 7, 2005

The directed three-dimensional self-assembly of microstructures and nanostructures through the selective hybridization of DNA is the focus of great interest toward the fabrication of new materials. Single-stranded DNA is covalently attached to polystyrene latex microspheres. Single-stranded DNA can function as a sequence-selective Velcro by only bonding to another strand of DNA that has a complementary sequence. The attachment of the DNA increases the charge stabilization of the microspheres and allows controllable aggregation of microspheres by hybridization of complementary DNA sequences. In a mixture of microspheres derivatized with different sequences of DNA, microspheres with complementary DNA form aggregates, while microspheres with noncomplementary sequences remain suspended. The process is reversible by heating, with a characteristic "aggregate dissociation temperature" that is predictably dependent on salt concentration, and the evolution of aggregate dissociation with temperature is observed with optical microscopy.

Introduction

The DNA double helix consists of two negatively charged phosphate−sugar polymer chains held together by hydrogen bonds between the base pairs on each chain. If the sequence of bases on two chains of single-stranded DNA (ssDNA) are complementary (or near complementary), the hydrogen bonding can overcome the electrostatic repulsion and the two ssDNA chains can come together (hybridize) to form double-stranded DNA (dsDNA). The two chains reversibly separate (denature or "melt") above a characteristic melting temperature between approximately 30 and 80 °C. The melting temperature increases with the length of the chain and the concentration of salt in solution and depends to a lesser extent on the specific sequence of base pairs.[1−3]

The melting and hybridization of DNA oligomers has been extensively investigated for many years,[4] initially with a focus on genetic detection.[5] During the past decade, DNA hybridization has also been exploited to build DNA nanostructures in solution[6−9] and to guide the self-assembly of DNA-derivatized nanostructures and microstructures.[10,11] In particular, DNA-derivatized gold nanoparticles have been assembled onto surfaces[12] or onto other nanoparticles to form nanoparticle aggregates.[13] The ability to independently control the specificity, strength, and separation of a connection,[14] as well as the melting temperature of bonds, make DNA a versatile tool in the quest for new 'smart' materials, and aggregation of DNA-derivatized gold nanoparticles by hybridization has been well explored. Because of their small size, however, characterization of DNA-only or DNA−gold nanoparticle structures is difficult and indirect: UV−vis absorption spectroscopy only yields averaged measurements, and transmission electron microscopy (TEM) observation is made difficult by the high-vacuum conditions of the measurement.

In this paper, we present a scheme for derivatizing larger polystyrene particles with DNA for the purpose of assembling colloidal aggregates. This larger, polystyrene system is compelling for a number of reasons. First, we can directly follow the dynamics of this larger system using optical microscopy in order to better understand and control the use of hybridization for guiding particle self-

* Author to whom correspondence should be addressed.
[†] Physics Department, California Polytechnic State University.
[‡] Chemical Engineering Department, University of California, Santa Barbara.
[§] Materials Engineering Department, California Polytechnic State University.
[£] Materials Department, University of California, Santa Barbara.
[∥] Present address: Materials Science and Engineering Department, University of Washington, Seattle, WA 98195.
[⊥] Present address: Department of Physics, New York University, 4 Washington Place, New York, New York 10003.

(1) SantaLucia, J. *Proc. Natl. Acad. Sci. U.S.A.* **1998**, *95*, 1460−1465.
(2) Owczarzy, R.; Vallone, P. M.; Gallo, F. J.; Paner, T. M.; Lane, M. J.; Benight, A. S. *Biopolymers* **1997**, *44*, 217−239.
(3) Owczarzy, R.; You, Y.; Moreira, B. G.; Manthey, J. A.; Huang, L. Y.; Behlke, M. A.; Walder, J. A. *Biochemistry* **2004**, *43*, 3537−3554.
(4) Wetmur, J. G. *Crit. Rev. Biochem. Mol.* **1991**, *26*, 227−259.
(5) Chee, M.; Yang, R.; Hubbell, E.; Berno, A.; Huang, X. C.; Stern, D.; Winkler, J.; Lockhart, D. J.; Morris, M. S.; Fodor, S. P. A. *Science* **1996**, *274*, 610−614.
(6) Seeman, N. C. *Nano Lett.* **2001**, *1*, 22−26.
(7) Seeman, N. C. *Sci. Am.* **2004**, *290*, 64−75.
(8) Shih, W. M.; Quispe, J. D.; Joyce, G. F. *Nature* **2004**, *427*, 618−621.
(9) Ekani-Nkodo, A.; Kumar, A.; Fygenson, D. K. *Phys. Rev. Lett.* **2004**, *93*, 268301.
(10) Bashir, R. *Superlattices Microstruct.* **2001**, *29*, 1−16.
(11) Niemeyer, C. M. *Appl. Phys. A: Mater. Sci. Process.* **1999**, *68*, 119−124.
(12) Schwartz, P. V. *Langmuir* **2001**, *17*, 5971−5977.
(13) Storhoff, J. J.; Elghanian, R.; Mucic, R. C.; Mirkin, C. A.; Letsinger, R. L. *J. Am. Chem. Soc.* **1998**, *120*, 1959−1964.
(14) Storhoff, J. J.; Lazarides, A. A.; Mucic, R. C.; Mirkin, C. A.; Letsinger, R. L.; Schatz, G. C. *J. Am. Chem. Soc.* **2000**, *122*, 4640−4650.

10.1021/la046790y CCC: $30.25
Published on Web 05/06/2005

assembly. Additionally, microspheres a few hundred nanometers in diameter can aggregate into structures with unique optical properties, such as colloidal crystals having stop band or complete band gaps in the optical range of the spectrum.[15] Last, the ability to tailor the size, shape, and internal chemistry (including the magnetic, optical, and electrical properties) of colloidal microstructures and nanostructures may make this a model system of self-assembling materials with programmable properties.

In 1987, Kremsky et al. reported an efficient two-step covalent process for attaching ssDNA to micrometer-sized polystyrene microspheres.[16,17] Since then, there have been numerous studies involving microspheres, but most of them have been focused toward biological purposes such as genetic detection, where DNA-coated microspheres in the presence of the target strand of DNA adhere either to DNA on other microspheres[18−20] or to a DNA-coated surface.[21]

To date, there have been only a few reports focused on using DNA to direct the self-assembly of micrometer-sized colloids for the purpose of developing new materials. Hartmann[22] studied the hybridization-mediated selective attachment of DNA-functionalized microspheres onto surface-anchored complementary DNA. Using a similar system, Zhang et al.[21] studied the effects of shear flow on the detachment of DNA-derivatized microspheres bound to a substrate via DNA hybridization. Some steps have also been taken toward the three-dimensional self-assembly of micrometer-sized particles in solution. Soto et al.[23] recently reported that two sets of ssDNA-coated microspheres with the size ratio properly chosen and linked together by hybridization can create octahedron and tetrahedron structures. Two years ago, Milam[24] fabricated and carefully characterized aggregates self-assembled from bi-disperse microspheres coated with complementary ssDNA. The size and shape of the aggregates were studied as a function of the DNA length and the salt concentration by optical and confocal microscopy. Recently, Valignat et al.[25] were able to assemble DNA-decorated microspheres into a predetermined arrangement using laser tweezers, and Biancaniello et al.[26] reported an annealed crystal of DNA-linked microspheres.

While Milam, Zhang, and Valignat attached the DNA to the microspheres through a NeutrAvidin−biotin link, Soto and Biancaniello chose to covalently attach the DNA onto the microspheres using carboxydiimide chemistry. Although technically more difficult and time-consuming, the covalent attachment has several advantages. First, the smaller molecular footprint of the amide linkage permits denser DNA surface coverage than is possible using the NeutrAvidin−biotin link, which has a much larger footprint due to the steric hindrance of its bulky proteins. Second, the amide linkage is more robust than the NeutrAvidin−biotin link, whose proteins can denature at high temperature and thus compromise the strength of the bonds. Third, an amide bond under tension is stronger than the DNA hybridization bond, in contrast to the NeutrAvidin−biotin link. Zhang reports that the bond made of a succession of NeutrAvidin−biotin and DNA hybridization broke at the NeutrAvidin−biotin connection when the force applied exceeded 2 pN,[21] whereas the force necessary to separate hybridized strands of antiparallel DNA from opposite ends is approximately 60 pN.[27,28]

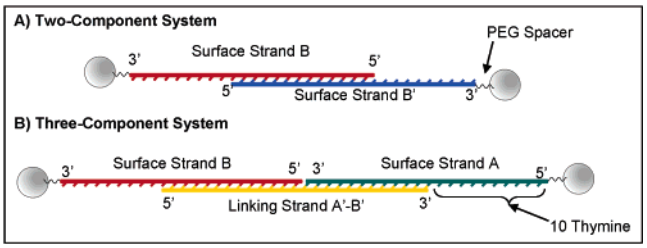

Figure 1. Attachment scheme for (a) the two-component system and (b) the three-component system.

The aim of this paper is to expand the work done with nanoparticles to polystyrene microspheres, promoting microspheres as DNA-guided building blocks. To this end, we functionalize two sets of microspheres with different sequences of ssDNA and subsequently link together the strands and, hence, the microspheres to which they are attached. We use two different DNA-linking motifs (see Figure 1 and Table 1). In the first, two complementary strands of ssDNA are attached to two different sets of identical microspheres; these complementary ssDNA strands are allowed to hybridize so that the microspheres are held together by a "two component" bond. In the second, two noncomplementary strands of ssDNA are attached to two different sets of microspheres. In this case, the ssDNA strands on the different sets of spheres are each complementary to opposite ends of a third free-floating ssDNA "linker"; this linker hybridizes with the ssDNA strands on different microspheres so that the microspheres are held together by a "3 component" bond.

For reasons discussed above, we have chosen to covalently link the DNA to the surface of the microspheres via carboxydiimide chemistry. A conjugation process (attachment of DNA to microsphere surface) was developed to minimize the tendency of the microspheres to nonspecifically bind (that is, to aggregate through forces other than hybridization of complementary ssDNA).

The method used to attach DNA results in a high surface density of DNA, which electrostatically and sterically stabilizes the microspheres in suspension. The density of DNA on the microsphere surface was estimated to be 20−50 times greater than that achieved with the NeutrAvidin−biotin link.[24] Therefore, extra measures taken by others to prevent nonspecific binding were not necessary, such as using microspheres with a high surface density of carboxyl groups that are rather difficult to synthesize (e.g., CML microspheres), or using bulky poly(ethylene glycol) (PEG) polymers.[23]

(15) Subramanian, G.; Manoharan, V. N.; Thorne, J. D.; Pine, D. J. *Adv. Mater.* **1999**, *11*, 1261−1265.
(16) Kremsky, J. N.; Wooters, J. L.; Dougherty, J. P.; Meyers, R. E.; Collins, M.; Brown, E. L. *Nucleic Acids Res.* **1987**, *15*, 2891−2909.
(17) Wolf, S. F.; Haines, L.; Fisch, J.; Kremsky, J. N.; Dougherty, J. P.; Jacobs, K. *Nucleic Acids Res.* **1987**, *15*, 2911−2926.
(18) Perrin, A.; Martin, T.; Theretz, A. *Bioconjugate Chem.* **2001**, *12*, 678−683.
(19) Bains, W. *Clin. Chem.* **1998**, *44*, 876−878.
(20) Bains, W. *Anal. Biochem.* **1998**, *260*, 252−255.
(21) Zhang, Y.; Eniola, A. O.; Graves, D. J.; Hammer, D. A. *Langmuir* **2003**, *19*, 6905−6911.
(22) Hartmann, D. M.; Heller, M.; Esener, S. C.; Schwartz, D.; Tu, G. *J. Mater. Res.* **2002**, *17*, 473−478.
(23) Soto, C. M.; Srinivasan, A.; Ratna, B. R. *J. Am. Chem. Soc.* **2002**, *124*, 8508−8509.
(24) Milam, V. T.; Hiddessen, A. L.; Crocker, J. C.; Graves, D. J.; Hammer, D. A. *Langmuir* **2003**, *19*, 10317−10323.
(25) Valignat, M. P.; Theodoly, O.; Crocker, J. C.; Russel, W. B.; Chaikin, P. M. *Proc. Natl. Acad. Sci.* **2005**, *102*, 4225.
(26) Biancaniello, P.; Kim, A.; Crocker, J. C. *Phys. Rev. Lett.* **2005**, *94*, 58302.
(27) The following reference reports how the DNA rupture force depends logarithmically on the speed of DNA separation and has been measured for 10 bp oligomers to be about 18 and 40 pN for speeds of 1 nm/s and 1μm/s, respectively. However, at the higher speeds dictated by the Browian Motion of our microspheres, the rupture force should approach the asymptotic limit for DNA of 60 pN.
(28) Strunz, T.; Oroszlan, K.; Schafer, R.; Guntherodt, H. J. *P. Natl. Acad. Sci. U.S.A.* **1999**, *96*, 11277−11282.

Table 1. DNA Sequences Used, from the 5′ End to the 3′ End[a]

strand name and function	sequence	T_m (°C)
strand A: surface strand	5′-/5AmMC6//iSp18/TTT TTT TTT TCG CAT TCA GGA T-3′	53.8
strand B′: surface strand	5′-TAC GAG TTG AGA TTT TTT TTT T/iSp18//3AmMC7/-3′	49.4
strand B: surface strand	5′-TCT CAA CTC GTA TTT TTT TTT T/iSp18//3AmMC7/-3′	49.4
strand A′−B′: linking strand	5′-TAC GAG TTG AGA ATC CTG AAT GCG-3′	49.4; 53.8
strand D: noncomplementary strand	5′-/5AmMC6//iSp18/TTT TTT TTT TTT GGC TAT GTA T-3′	NA

[a] T = thymine, A = adenine, C = cytosine, and G = guanine. iSp18 signifies a PEG spacer used for steric freedom,[29] 5AmMC6 is the amine attachment point at the 5′ end, and 3AmMC7 is the amine attachment functional group at the 3′ end of DNA. Each surface strand sequence contains 10 T bases designed to improve DNA packing and microsphere electrostatic stability.[30] The hybridizing sequence of each oligomer is underlined, and its melting temperature in °C ± 1.4 °C, calculated from the nearest-neighbor method[1,2] for a 200 μm DNA concentration and 50 mM NaCl is given in the right column.

The specificity of the resulting DNA-guided self-assembly process is also demonstrated in experiments where spheres are observed to bind only to spheres with complementary strands and not to spheres with noncomplementary strands.

Consistent with normal DNA behavior, the DNA-linked aggregates disperse completely when the temperature is raised past a characteristic aggregate dissociation temperature, T_d. The microspheres reaggregate when the samples are allowed to cool below T_d. The aggregate dissociation temperature, T_d, is determined by optically observing aggregate dissociation and increases with increased concentration of sodium ions, consistent with the melting temperature of free-floating DNA. Interestingly, we find that the dissociation temperature for the two-component system is higher than that of the three-component system. We also find that the dissociation transition for the aggregates is 10 times more abrupt than the melting transition of unattached DNA in solution.[1,2]

Experimental Methods

Reagents and Equipment. The following solutions were made on site: 10 mM, pH 7.5 phosphate-buffered solution (PBS), 2% Tween-20 PBS solution, 10 mM, pH 7.5; and solutions of 1-ethyl-3-(3-dimethylaminopropyl) carbodiimide hydrochloride (EDC) in 10 mM, pH 4.5 2-morpholinoethanesulfonic acid (MES) buffer with a concentration of 10 mg/mL.

Carboxyl-modified divinylbenzene (DVB) cross-linked polystyrene latex microspheres, with carboxyl functional groups on the surface, were purchased from Interfacial Dynamics Corporation (Portland, OR). White and fluorescent microspheres were ordered with the following identical parameters. Each has a diameter of 0.97 μm and a surface density of carboxylic groups of 1.075×10^{18} COOH/m^2 (corresponding to 3.16×10^6 groups per particle and a molecular footprint of about 1 nm^2). The fluorescent microspheres have an excitation wavelength of 520 nm and an emission wavelength of 580 nm.

The oligonucleotides are synthesized by Biosearch Technologies (Novato, CA) and Integrated DNA Technologies, Inc. (Coralville, IA). The DNA sequences have been previously used to aggregate gold nanoparticles[13] and to bind gold nanoparticles to surfaces.[12] Five sequences were used in this study: four 22-base surface-bound strands and a 24-base linker (Table 1).

Microsphere Preparation. The polystyrene spheres come dispersed in distilled deionized water. They were sonicated and vortexed for 15 s and subsequently centrifuged at 2200*g* for 15 min. The supernatant was then replaced with MES buffer, enough to make the solution 1% solid by volume. The above washing process was repeated and the samples were vortexed and then sonicated repeatedly to disperse any remaining groups of microspheres.

Conjugation of Microspheres. Prior to use, the EDC was stored at −20 °C in a water-free environment. The EDC solution was used immediately, and the excess solution discarded. Microspheres prepared in MES buffer (MES is always 10 mM, pH 4.5) and DNA (178.6 pM/cm^2 of microsphere surface was typically used. However, we were able to decrease the DNA concentration by a factor of 4 with no measurable decrease in DNA surface density on the microspheres) were placed in a 1.5 mL microfuge tube. Fresh solution (30 μL) of EDC (10 mg/mL) in MES buffer was added to the sample and incubated at 25 °C for 30 min while being agitated. After 30 min, another 30 μL of fresh EDC/MES solution was added to the sample and agitated for an additional 30 min. The sample's volume was then doubled by adding the same amount of 2% Tween-20 MES buffer as there was solution. Enough ammonium hydroxide was added to make the solution 4% ammonium hydroxide by volume. Then, the microspheres were washed three times in PBS with the following process: (1) Samples were sonicated and vortexed, each for less than 10 s, and centrifuged at 2200*g* for 15 min. (2) The supernatant was removed and replaced with PBS to make the solution 1% solid by volume. (3) The samples were sonicated and vortexed (less than 10 s each) until the DNA-covered microspheres were fully dispersed in solution. After the above wash cycle was repeated three times, the resulting DNA-derivatized microspheres, dispersed in PBS to 1% solid by volume, were stored at 7 °C.

Amino-modified ssDNA attaches to carboxyl-modified microspheres by means of an amide bond, activated by water-soluble EDC (Figure 2). In control experiments without EDC, it was found that fluorescently labeled DNA did not attach to the beads, indicating that, when EDC is used, the DNA is covalently attached to the microspheres and not simply physisorbed onto the polystyrene surface. The EDC forms a nucleophile-reactive intermediary with the carboxyl group on the microsphere surface, which subsequently forms an amide bond with the functional amino group on the ssDNA. Urea is produced as a byproduct (not shown in Figure 2).

Prior to being dispersed in the MES buffer solution, the microspheres are stabilized in aqueous suspension at pH 7 through the electrostatic repulsion provided by the surface COO^- groups. The pK_a of the COOH on the particles is approximately 5, so the particles lose much of their charge when placed in the pH 4.5 MES buffer solution, causing them to aggregate mildly. The aggregates are readily broken apart by mild agitation or sonication but reaggregate when the agitation ceases. As conjugation of the spheres with DNA proceeds, the aggregates tend to break apart under mild agitation, but in this case, they stay apart when the agitation ceases. The microspheres are thus observed to be better stabilized after conjugation with DNA, which we attribute to the increased charge, as well as the steric repulsion provided by the DNA chains.

Aggregation of Microspheres via DNA Hybridization. All hybridization experiments were carried out in PBS [10 mM, pH 7.5], initially with a sodium ion concentration of $[Na^+] = 62.5$ mM. Two-component aggregates were created by mixing strand B′ microspheres and strand B microspheres together at 0.5% volume fraction of solid and left gently vibrating in the dark for at least a day at 7 °C. Three-component aggregates were created by first mixing the A microspheres with an excess of the A′−B′ ssDNA linker strands. The samples were left at 7 °C in the dark for 24 h on a vibrating table and then washed in PBS to dispose of excess linker strands. The hybridized spheres were resuspended in PBS at a volume fraction of 1% solid. Then strand A microspheres with hybridized A′−B′ linker were mixed with strand B microspheres. After the samples were incubated for only a few hours, aggregates form in both samples and begin to fall out of solution and rest at the bottom of the microfuge tubes. One to four days is allotted for the incubation process allowing for the formation of many macroscopic aggregates containing up to 10^9 microspheres.

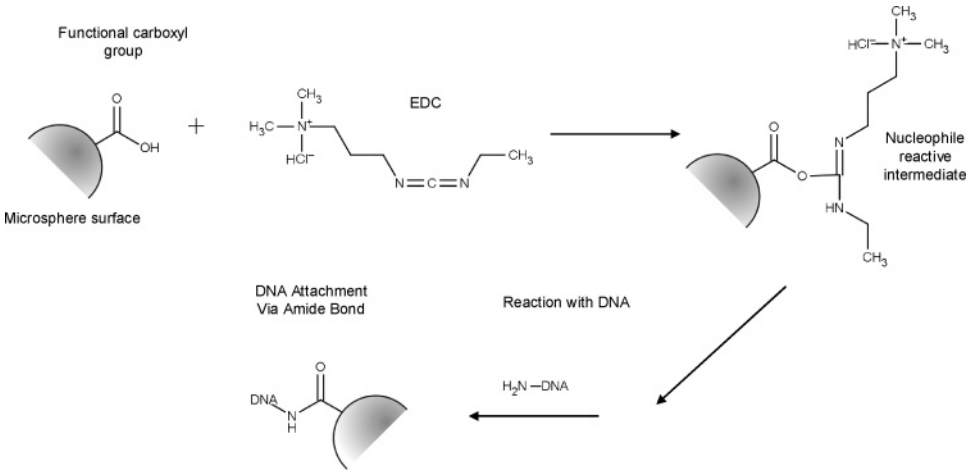

Figure 2. Mechanism for attaching amino-modified oligonucleotide to carboxyl-functionalized microspheres.

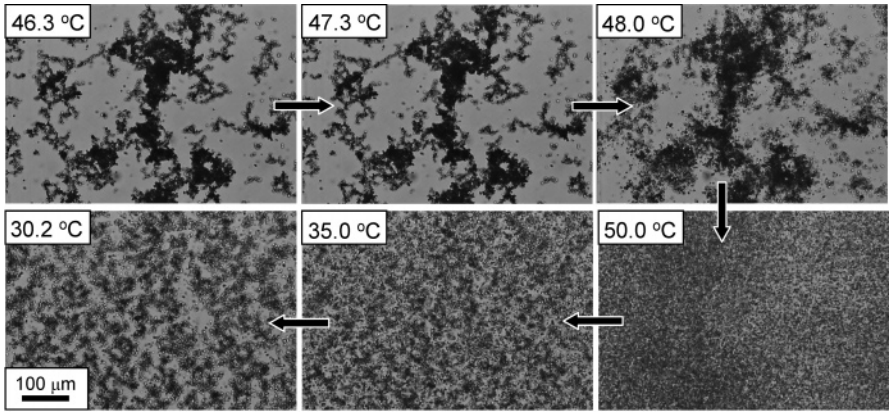

Figure 3. Dissociation and reaggregation of a two-component aggregate at 70 mM [Na+]. Top Left: the beginning aggregate below dissociation temperature. Following the arrows, the sample is heated above the dissociation temperature (T_d = 47.3 °C) and then allowed to cool. See Figures 4 and 8 for the mean gray intensity measurements and temperatures.

DNA Surface Density and Hybridization Efficiency. Fluorescence measurements and flow cytometry were used to determine the density of attached and/or hybridized DNA on the microsphere surface. For these experiments, DNA oligonucleotides identical to those described in Table 1, but labeled with fluorescent dyes, were purchased. Strand B′ was labeled with a Cy5 dye at its 5′ end, while the linker strand A′−B′ was labeled at its 3′ end with a 6FAM dye, a close derivative of fluorescein. For the fluorescence measurements, a calibration curve was first established with the fluorescent DNA in solution (no microspheres). The measurements of the amount of DNA covalently attached to the microspheres were then performed indirectly on the supernatant obtained after each washing step of the conjugation process. The DNA molar concentration obtained was then compared to that added initially to the microspheres. The difference of these two numbers gives the amount of DNA attached to the microspheres.

Direct measurements where performed, using a FACSAria flow cytometer (Becton Dickinson, San Jose, CA). To determine the surface density of DNA, microspheres derivatized with Cy5-dyed B′ strand were prepared following the standard protocol described above. To test the hybridization efficiency, a 6FAM dyed linker was hybridized onto microspheres derivatized with DNA (not dyed). The hybridization was performed at 100 mM [Na^+] in PBS buffer. Measurements from both of these samples were compared to reference (negative) samples consisting of microspheres alone and microspheres derivatized with DNA that was not dyed. The fluorescence intensity for each dye was calibrated using Quantum PE-Cy5 and Quantum FITC calibrations beads purchased from Bangs Laboratories. From these calibration curves, the number of molecules of equivalent fluorochrome (MESF, i.e., the mean number of attached or hybridized DNA for each sample) was calculated. It should be noted that these measurements can only yield an estimate of the DNA loading and efficiency of hybridization because the PE-Cy5 dye of the calibration beads and the Cy5 dye of the DNA are slightly different and because the quantum yield extinction coefficient of a dye almost always changes when it is attached onto a DNA strand.[31] Nevertheless, the same calibration method has been used by others,[21] so that our data can be directly compared to that reported in those studies.

Measurement of Dissociation Temperature. The DNA-mediated aggregates dissociate when heated above some characteristic temperature, T_d, which we designate as the aggregate dissociation temperature. This dissociation temperature is closely related to the melting temperature, T_m, of free floating DNA, but is expected to be somewhat higher because of cooperative effects, which we discuss later.

The aggregate dissociation temperature, T_d, was measured as a function of sodium ion concentration [Na^+] using the following procedure: 1.0 μL of aggregate and aqueous buffer was removed from the bottom of the microfuge tube and placed in a cell with 110 μL of PBS of *varying ionic strength*. Aggregates were observed using an optical microscope, while the temperature was monitored with a submerged thermal couple. Aggregates were then heated until they dissociated (see Figure 3).

The temperature was increased at 0.5 °C/min, and images of the dissociation were taken for the entire aggregate dissociation process. Prior to dissociation, the screen appears mostly bright with some black patches where aggregates reside. As the aggregates dissociate, the screen becomes darker as particles

(29) *Technical Bulletin: Amino-Modified Custom Oligonucleotides*; IDT: Coralville, IA, 2001.
(30) Storhoff, J. J.; Elghanian, R.; Mirkin, C. A.; Letsinger, R. L. *Langmuir* **2002**, *18*, 6666−6670.
(31) *DNA Technical Note: Fluorescence Excitation and Emission*; IDT: Coralville, IA, 2001.

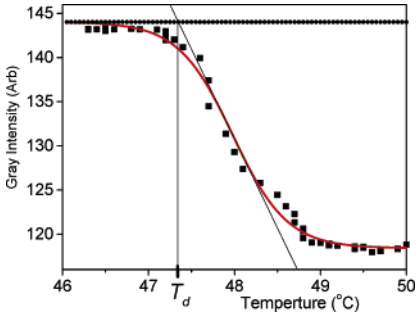

Figure 4. Analysis method for determining aggregate dissociation temperature, which is found to be 47.3 °C for the data presented in Figure 3. The red line is a fit with a sigmoidal function. The dissociation temperature, T_d, is the temperature of the point of intersection of the upper horizontal line determined using the sigmoidal fit and the line fit to the curve at the point of inflection of the sigmoid. Not all data points have been shown in the figure for clarity.

spread out, eventually covering the entire field of view and dimming the overall intensity of the screen. Therefore, a convenient measure of the progression of the dissociation process is the mean gray intensity, i.e., the average pixel brightness across the screen. The mean gray intensity was calculated for each image taken at different temperatures and the points were plotted as a function of temperature (Figure 4).

The data were then fit to a sigmoidal function. The dissociation temperature, T_d, was taken to be the point of intersection between the horizontal line in Figure 4 corresponding to the asymptotic measured intensity at low temperatures and the line fit to the curve at the point of inflection (halfway between the low- and high-temperature asymptotic intensities). Physically, the micrographs show that this is the lowest temperature at which the outermost microspheres of the aggregates start to move away from the aggregates and the dissociation becomes detectable in the low-magnification (×20) optical micrographs.

The uncertainty in measured temperature is estimated to be 1 °C due partially to the separation (~1 cm) between the observed aggregate and the temperature sensor and also due to the time needed for the temperature to reach equilibrium at the center of the circular observation window in the heating stage (diameter ≈ 0.6 mm), which was estimated to be about 1 min. It should also be noted that T_d exhibited a small dependence on the heating rate (T_d increases by 2.75 °C when the heating rate is lowered from 5 to 0.25 °C/min). However, our goal in this study is not to provide a precise measurement of T_d but rather to critically assess the specificity of the interaction that binds the microspheres, as well as to obtain an empirical working dissociation temperature for characterizing annealing experiments.

Results and Discussion

DNA Surface Density and Hybridization Efficiency. The fluorescence measurements yielded a density of DNA on the microsphere surface of $1.9 \times 10^5/\mu m^2$ with about an 18% uncertainty, corresponding to a DNA molecular footprint of about 5.3 nm^2 or about 5.5×10^5 DNA strands/bead. The flow cytometry experiments gave numbers that were lower but consistent with this surface coverage: the very sharp peak shown on the count vs fluorescence intensity histogram of Figure 5 corresponds to more than 2×10^5 DNA strands/bead, i.e. a density of $6.7 \times 10^4/\mu m^2$ or a DNA molecular footprint of about 15 nm^2. Even using the lower of the two values, the DNA surface density is nearly 20 times greater than that achieved using the Neutravidin−biotin link (3.25×10^3 molecules/μm^2 reported in ref 24), which presumably was limited by the surface density of active sites of the Neutravidin on the bead surface of $4.6 \times 10^3/\mu m^2$.

By contrast, the number of hybridized strands, as determined by flow cytometry, is quite low: approximately 6500 strands per bead, which corresponds to a surface coverage of 2200 linkers/μm^2. The distribution of hybridized strands has a broader peak (relative to the mean) than that of the surface-bound DNA (Figure 5), consistent with the expectation that the width of the distribution should scale with the square root of the mean number of hybridized strands. We estimate the hybridization efficiency (fraction of attached DNA hybridized with a linker) to be approximately 3.25%. This number is low but is consistent with the high surface density of attached DNA. Others have reported that the hybridization efficiency of a 25 bp target strand onto its complementary sequence, immobilized onto a gold surface and performed at 1M NaCl, decreases from 70% to 10% when the surface density of attached DNA increases from 2×10^4 to 1.2×10^5 strands/μm^2).[32] Additionally, it is possible that some DNA strands may be attached to the microsphere surface via a group other than the intended terminal amine, which would render the attached DNA unable to hybridize. This unintended attachment might result from the high reactivity of the acidic environment (pH 4.5) during conjugation.[33]

In any case, the DNA-derivatized beads were observed to be excellently stabilized in suspension. The flow cytometry experiments additionally showed that more than 95% of the colloids present in a sample after conjugation are individual microspheres: the beads did not bind to other microspheres unless through hybridization of complementary sequences of DNA.

Selectivity Experiments. The aggregation of DNA-linked microspheres is selective, owing to the sequence sensitivity of DNA hybridization. To investigate the specificity of the bonds between the microspheres in our system, red fluorescent microspheres functionalized with a noncomplementary DNA sequence D were added during the assembly of DNA-linked aggregates made of undyed microspheres using both the two- and three-component systems. The microspheres were mixed in PBS with equal parts dyed and undyed microspheres for a total microsphere concentration of 1 vol%. The mixture was slowly rotated overnight in order to prevent the settling of microspheres on the bottom of the microfuge tubes and the inevitable entrainment and trapping of nonhybridizing red microspheres within the matrix of DNA-linked microspheres. After overnight rotation, the suspension consisted of perfectly dispersed red microspheres (appearing bright in Figure 6) and undyed aggregates (appearing dark) devoid of the red spheres with the noncomplementary DNA sequence. Although it may appear as if some red microspheres are bound to each other, real-time observations reveal that they are moving past each other. Therefore, we conclude that the fraction of nonspecifically bound microspheres is essentially zero.

Role of Surfactant in Nonspecific Binding. It was found that the addition of Tween-20 at the end of the conjugation step enhances the ability of the aggregates to disperse upon heating. If Tween-20 is not used, a small core at the center of an aggregate may fail to disperse upon heating; including Tween-20 allows the complete dissociation of the aggregate upon heating. Other than enhancing the dissociation of aggregate cores, we observed no effect of the Tween-20 on aggregate formation or dissociation. For example, flow cytometry measurements showed that nonspecific binding of colloids prior to aggregate formation is insignificant, whether Tween-20 is included or not. The detailed influence of the conjugation

(32) Peterson, A. W.; Heaton, R. J.; Georgiadis, R. M. *Nucleic Acids Res.* **2001**, *29*, 5163−5168.
(33) Rose, S. IDT, personal communication.

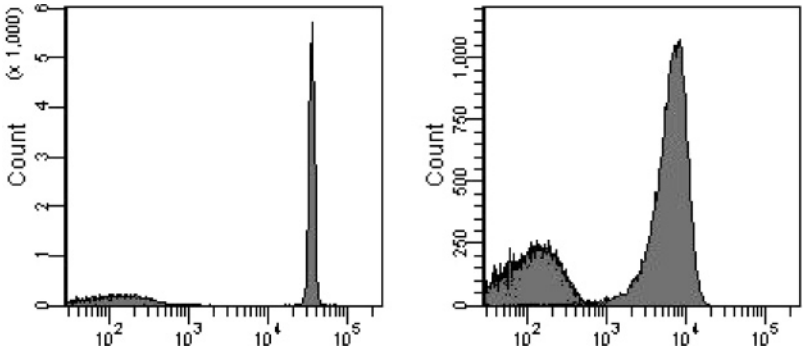

Figure 5. Flow Cytometry histograms: bead count (vertical axis) versus fluorescence intensity (horizontal axis). At left, bead count is shown as a function of the fluorescence intensity of the Cy5-dyed DNA surface strand, B′. The right histogram shows the bead count as a function of the fluorescence intensity of linker A′−B′ dyed with 6FAM dye hybridized onto (undyed) DNA covalently bound to the microspheres. Because the fluorescence of Cy5 is not the same as 6FAM, a direct comparison of the intensities of the two graphs does not yield the ratio of the associated populations of DNA on the microsphere surface.

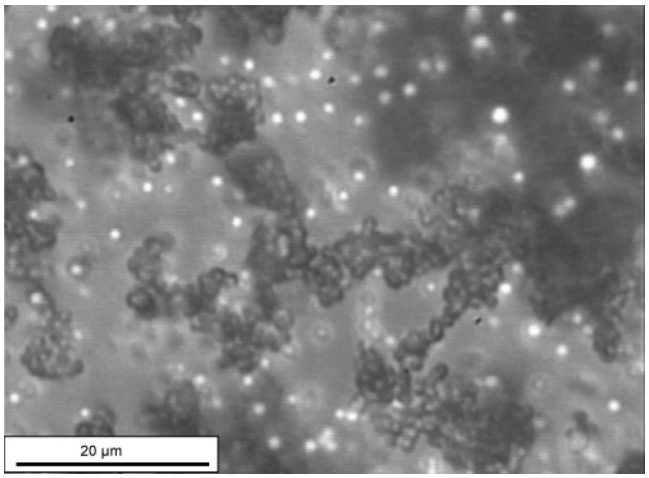

Figure 6. White microspheres of complementary two-component system (appear dark) were mixed with fluorescent red microspheres of noncomplementary strand D (appear bright).

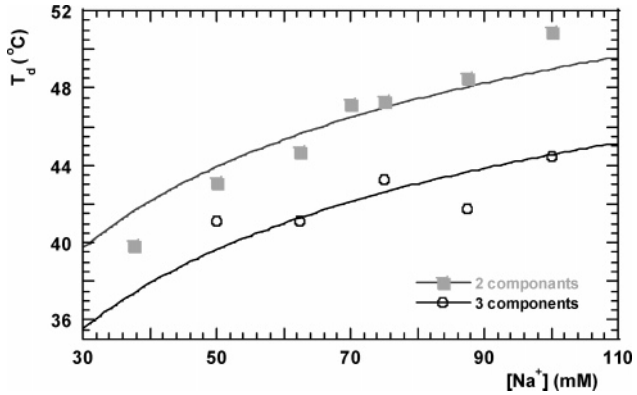

Figure 7. Dissociation temperature versus ionic strength for both three- and two-component aggregates. The full lines are a fit of the data points with eq 1, with one free parameter, the dissociation temperature at 50 mM Na^+.

protocol on the prevention of nonspecific binding and on the ability of the aggregates to disperse upon heating is not completely understood and is still under investigation. However, we offer some preliminary observations about nonspecific aggregation and how it may be prevented with Tween-20.

Nonspecific binding can occur when the surfaces of adjacent microspheres come close enough for the electrostatic repulsion to be overcome by van der Waals forces or by the attractive interactions between hydrophobic patches on microsphere surfaces. As observed in our experiments, replacing carboxyl groups with 22-base DNA strands greatly decreases nonspecific binding by both increasing the charge on the microsphere surface and providing steric repulsion by means of the DNA strands. Even this improved stabilization can fail when the microsphere surfaces are compressed together at the center of an aggregate of hybridized microspheres. For samples prepared with Tween-20, however, the aggregates disperse completely upon heating above T_d.

Tween-20 consists of a polar headgroup attached to three strands of PEG (averaging about 3 nm in length) and a hydrophobic 11-carbon alkyl chain. One possibility is that the hydrophobic alkyl chains bind to hydrophobic patches on the microsphere surfaces, effectively rendering those patches hydrophilic because of the PEG strands that are presented to the outside. The floppy PEG arms may also increase steric repulsion, although we note that the PEG strands on the Tween-20 are shorter than the ssDNA strands, so that they do not get in the way of hybridization between ssDNA strands on different spheres. Others have found[34] that PEG alone can stabilize polystyrene microspheres if the chains are more than 30 nm long.

Dependence of Aggregate Dissociation Temperature on Salt Concentration. The specificity of the bonds linking the microspheres was also assessed by heating the aggregates in buffers of varying ionic strength. If they are bound by hybridized DNA, the aggregates should dissociate when the DNA-mediated aggregates are heated above the aggregate dissociation temperature, T_d, as discussed earlier. Moreover, T_d should vary with the sodium ion concentration and exhibit a dependence similar to that observed for the melting of neat DNA. This procedure also allowed us to assess the relative merits of different conjugation and hybridization protocols as discussed in the previous section about surfactant.

Aggregate dissociation temperatures were measured for the three-component aggregates and two-component aggregates for a range of ionic strengths. The experimental data are reported in Figure 7. The figure also shows an empirical relationship describing the variations of T_m with NaCl concentration for free floating oligomers:[3]

$$\frac{1}{T_{m(1)}} = \frac{1}{T_{m(2)}} + (4.29n_{GC} - 3.95) \times 10^{-5} \ln\left(\frac{[Na^+]_2}{[Na^+]_1}\right) + 9.40 \times 10^{-6}(\ln^2 [Na^+]_2 - \ln^2 [Na^+]_1) \quad (1)$$

where n_{GC} is the number of G and C bases divided by the

(34) Kim, A.; Manoharan, V. N.; Crocker, J. C. *J. Am. Chem. Soc.* **2005**, *127*, 1592.

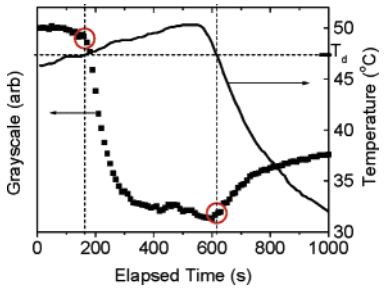

Figure 8. Mean gray intensity (squares) and temperature (line) for the dissociation and reaggregation for the data presented in Figure 3. Circled data points correspond to 47.3 °C, the aggregate dissociation temperature.

total number of bases of the oligomer and $T_{m(i)}$ are the melting temperatures in Kelvin for the corresponding sodium ion molar concentrations $[Na^+]_i$.

The functional form of eq 1, which gives the temperature dependence of the melting curve that was empirically derived for *free-floating* DNA, fits our data for the dissociation of the microsphere aggregates reasonably well, considering that the precision of the measurement is estimated to be ±1 °C. The agreement of measured dissociation temperatures of the aggregates in both systems with the general trend of the free-floating DNA melting behavior gives further evidence of the specificity of the force holding the microspheres into aggregates.

The essential difference between the two- and three-component systems is that linker is required to bind spheres together in the three-component system but not in the two-component system. In the three-component system, entropy favors the complete delocalization of the linker molecules throughout the solution, while aggregation requires that the linker molecules be localized between spheres. The entropic penalty associated with confining the linker between two microspheres leads to a dissociation temperature of the three-component system that is lower than that of the two-component system, where no such penalty exists (because all the DNA is permanently bound to the spheres).

Reversibility. Consistent with the reversible nature of DNA hybridization, DNA-linked aggregates, after dispersion, can be reassembled. The sequence of images in Figure 3 and the graph in Figure 8 demonstrate that, after dissociation, the microspheres again reassemble if the temperature is lowered below the aggregate dissociation temperature, T_d. The temperature at which the microspheres start to reaggregate is found to be close to T_d, the temperature at which the aggregates start to dissociate. It should be noted that the rate of microsphere dispersion does not increase with increased ramping rate of the temperature (see Figure 9). Instead, dispersion is controlled by the diffusion rate of the microspheres, which is very slow compared to the diffusion and the dissociation rate of the DNA. So, while the melting of the DNA is an equilibrium process, the dispersion and reaggregation of the microspheres is not at equilibrium at the relatively rapid temperature ramping rates (0.5 °C/min) of these experiments.

Sharpness of Dissociation Profile

The dissociation of DNA-linked microspheres is found to be a much sharper transition than the melting transition of the associated neat DNA dissolved in PBS. The sharpness of the transition can be quantified using the full width at half-maximum (fwhm) of the derivative of the gray scale heating curve. As noted above, the rate of

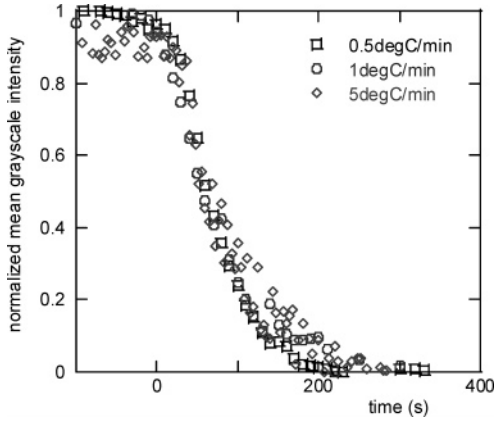

Figure 9. Normalized mean gray intensity versus time for the dissociation of a two-component aggregate at 70 or 75 mM Na^+ concentration. The time $t = 0$ has been set for $T = T_d$. The rate of microspheres dispersion does not increase when the ramping rate of temperature is increased from 0.5 up to 5 °C/min.

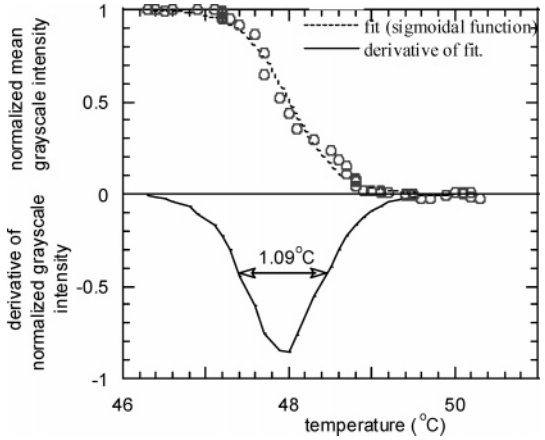

Figure 10. Normalized mean gray intensity versus temperature for the dissociation of a two-component aggregate at 70 mM Na^+ concentration. The dotted line is a fit of the data with a sigmoidal function. The full line is the derivative of this fit, showing the fwhm.

dissociation of an aggregate is limited by the diffusion of microspheres. In an effort to maximize the sharpness of the dissociation transition, the temperature should ramp slowly, so that aggregates dissociate under conditions as close as possible to equilibrium. Figure 10 shows the dissociation of a two-component aggregate where the temperature was increased at 0.5 °C/min. The derivative of the curve is also shown and yields a fwhm of 1 °C. Three-component aggregates also displayed a narrow dissociation transition, and within the accuracy of the data, we were not able to distinguish a difference in the fwhm between the two-component and three-component motifs. Other researchers measured a fwhm = 4 °C for the dissociation of gold nanoparticles linked by a three-component system using 15 bp DNA, while the melting curve for the associated *free-floating* DNA had a fwhm = 12 °C.[35] A narrower melting transition results in the ability to determine the DNA melting point with greater resolution. As a consequence, a DNA detection scheme based on aggregation of DNA-covered gold nanoparticles would be more selective for single-base mismatches than that of free floating DNA. Similarly, a DNA detection scheme based on aggregation of our DNA-derivatized microspheres should be considerably more selective than the scheme

(35) Elghanian, R.; Storhoff, J. J.; Mucic, R. C.; Letsinger, R. L.; Mirkin, C. A. *Science* **1997**, *277*, 1078−1081.

based on DNA-derivatized gold nanoparticles. At the same time, this sharp dissociation transition of DNA-derivatized microspheres makes a very challenging task of annealing DNA-derivatized microspheres into a lowest-energy configuration.

The cause of the increased sharpness of the dissociation profile for particles compared to the melting profile of DNA can be understood by considering the number of DNA strands involved in each dissociation process (although recent computer model results[36] indicate that modulation in local salt concentration may contribute to the sharpness of the dissociate profile). Many DNA strands must collectively unbind for two microsheres to dissociate, while fewer must unbind for two nanoparticles to dissociate, and fewer still (one, in fact) must unbind for two ssDNA strands to dissociate. Since particles remain bound until all strands collectively unbind, the transition will be sharper (and take place at a higher temperature) when more strands are involved. This is a cooperative effect that is well known: the larger the number of interacting units involved in a transition, the sharper the transition, whether those units are the molecules in a boiling liquid, the base pairs in a DNA chain, or as in this case the hybridizing ssDNA strands themselves. Therefore, we expect the transition to be broadest for two hybridizing strands, narrower for ssDNA attached to nanoparticles, and narrower still for microspheres, which involve the greatest number of hybridizing ssDNA strands.

Conclusions

We have developed a protocol for covalently attaching ssDNA to carboxylated (not CML) polystyrene latex microspheres that can be used to controllably and reversibly assemble large aggregates of microspheres with excellent selectivity. The excellent stability of the microspheres is the result of the high surface density of DNA achieved on the microspheres through carboxydiimide chemistry, which is performed at low pH. The aggregates reversibly and completely dissociate at a characteristic temperature, which increases with increased concentration of $[Na^+]$ consistent with the melting temperature of free DNA in solution. The existence of multiple bonds between microspheres results in a dissociation transition that occurs much more abruptly and at a higher temperature than the melting transition of the associated free-floating DNA in solution. These results highlight DNA as an excellent selective nanoscopic adhesive to guide the assembly of tailored materials.

Acknowledgment. We gratefully acknowledge fruitful conversations with Eric J. Kantorowski (Cal Poly Chemistry), assistance and insight from Khodadad N. Dinyari and Michael Chi-Hang Yeung, and conversations with Richard Owczarzy.[2,3] We also thank Karen Y. Dane of the Chemical Engineering Department at UCSB who conducted and helped analyze the flow cytometry measurements. This work was supported in part by the Department of the Navy, Office of Naval Research, under Award No. N00014-04-1-0436, in part by the National Science Foundation under Grant No. CTS-0221809, and in part by Raytheon Corporation.

LA046790Y

(36) Jin, R.; Wu, G.; Li, Z.; Mirkin, C. A.; Schatz, G. C. *J. Am. Chem. Soc.* **2003**, *125*, 1643.